THE ASTROPHYSICAL JOURNAL, 436:L169–L172, 1994 December 1

A DIRECT IMAGE OF WIND INTERACTION IN THE POST–AGB EVOLUTION: CO OBSERVATIONS OF M1-92

V. BUJARRABAL,[1] J. ALCOLEA,[1] R. NERI,[2] AND M. GREWING[2]
Received 1994 July 12; accepted 1994 September 13

ABSTRACT

We present high-resolution CO $J = 1$–0 maps of the protoplanetary nebula M1-92, Minkowski's Footprint, obtained with the IRAM interferometer at Plateau de Bure. The cartography is particularly revealing. Three components are distinguished in the maps: a bipolar outflow, with a (deprojected) velocity of ~ 65 km s^{-1}, a hollow prolate structure, with an axial velocity increasing with the distance to the star up to ~ 60 km s^{-1}, and a central condensation with velocities smaller than 10 km s^{-1}. A remarkable continuity in position and velocity is found between the hollow component and the bipolar flow. We argue that these properties indicate that an important dynamical interaction between both features is active at the present moment and affects most of the nebular material. Such an interaction would consist in a significant momentum transport from the bipolar fast flow to the rest of the nebula.

Subject headings: circumstellar matter — stars: AGB and post-AGB — planetary nebulae: individual (M1-92)

1. INTRODUCTION

M1-92, Minkowski's Footprint, is a proto–planetary nebula (PPN) that has been observed in detail in the optical and IR (e.g., Herbig 1975; Calvet & Cohen 1978). The temperature of the central star is $\sim 20{,}000$ K, this object being therefore in an intermediate state of evolution as PPN; its total luminosity and distance have been estimated to be $\sim 10^4\ L_\odot$ and 3 kpc, respectively (Calvet & Cohen 1978; see also Solf 1994). The optical image has a typical angular extent of $\sim 10''$ (5×10^{17} cm), and consists of two lobes defining a conspicuous axis of symmetry. The orientation of this axis in the plane of the sky is approximately northwest–southeast; it is also probably inclined with respect to the plane of the sky, the NW lobe pointing toward the observer. This symmetry and its orientation are confirmed by the high-velocity bipolar outflow detected by optical spectroscopy (Herbig 1975; Solf 1994), that shows expansion velocities between 200 and 500 km s^{-1}. The existence of a gap between the two lobes and the high obscuration toward the central star suggest the presence in the center of the nebula, and perpendicular to the axial flow, of an oblate dust condensation. In fact, a torus-like structure has been inferred from IR color index images (Eiroa & Hodapp 1989). M1-92 also presents OH maser emission, which indicates that this object is O-rich. The OH 1667 MHz line has been mapped with high spatial resolution by Seaquist, Plume, & Davis (1991), showing a velocity-position structure in which the blue peak arises from the southeast and the red emission comes from the northwest, opposite to the fast flow detected in the optical lines. This suggests that the OH maser is formed in a flat, compact component, perpendicular to the symmetry axis. The size of this OH structure (3″–4″) is only slightly larger than Eiroa & Hodapp's ring (2″–3″), and probably corresponds to the same torus-like condensation.

We present here CO high-resolution observations obtained with the IRAM interferometer at Plateau de Bure. As we will show, the CO observations probe the bulk of the nebular material, and most of the gas is molecular. All the components of the envelope are clearly represented in our data, including the torus and bipolar flow. Even more interestingly, a clear interaction between the different winds is detected by means of a gradual increase of the expansion velocity from the central condensation to the bipolar fast clumps.

2. OBSERVATIONS AND DATA REDUCTION

We have carried out observations of M1-92 in the ^{12}CO $J = 1$–0 line, at 2.6 mm wavelength, using the IRAM interferometer located at the Plateau de Bure (French Alps), during the winter of 1993–1994. The instrument consists of four antennas of 15 m diameter, equipped with SIS heterodyne receivers. Other characteristics of the array have been described in detail by Guilloteau et al. (1992). The observations were done using five different configurations for the telescopes, the resulting *uv* coverage is shown in Fig. 1 (Plate L10). The corresponding synthesized "dirty" beam (Fig. 1) has the largest negative (positive) sidelobes at a level of -9.6 dB (-7.7 dB) with respect to the maximum. At half-power, the dirty beam has major and minor axes of 2.″4 and 1.″6, respectively, the major axis being at a position angle (P.A.; from north to east) of 29°. As backend we used a digital correlator divided in 128 channels of 0.625 MHz each, though the visibilities were averaged to a velocity resolution of 3.25 km s^{-1}.

Pass-band calibration was corrected by observing strong quasars (3C 345 and 3C 273) once or twice per configuration. Phase calibration was performed by observing a (structureless) nearby quasar, 2013+370 (R.A.$_{J2000}$ 20:15:28.710; Decl.$_{J2000}$ 37:10:59.69), typically every 25–30 minutes. Amplitude calibration was done assuming for 2013+370 a flux of 3.75 Jy. The *uv* data were Fourier transformed and then CLEANed using the Högbom method. For restoring, we adopted a Gaussian "clean" beam with half-power shape equal to that found for the dirty beam. The final CLEANed maps for the channels where emission is found are shown in Figure 1. In these false-color maps, the spatial units are offsets in arcseconds with respect to the assumed position for the central star (R.A.$_{J2000}$ 19:36:18.90; Decl.$_{J2000}$ 29:32:49.9), and the intensity units are

[1] Centro Astronómico de Yebes (IGN), Apartado 148, E-19080 Guadalajara, Spain; bujarrabal,alcolea@cay.es
[2] IRAM, 300 rue de la Piscine, F-38406 St Martin d'Hères, France; neri,grewing@iram.fr

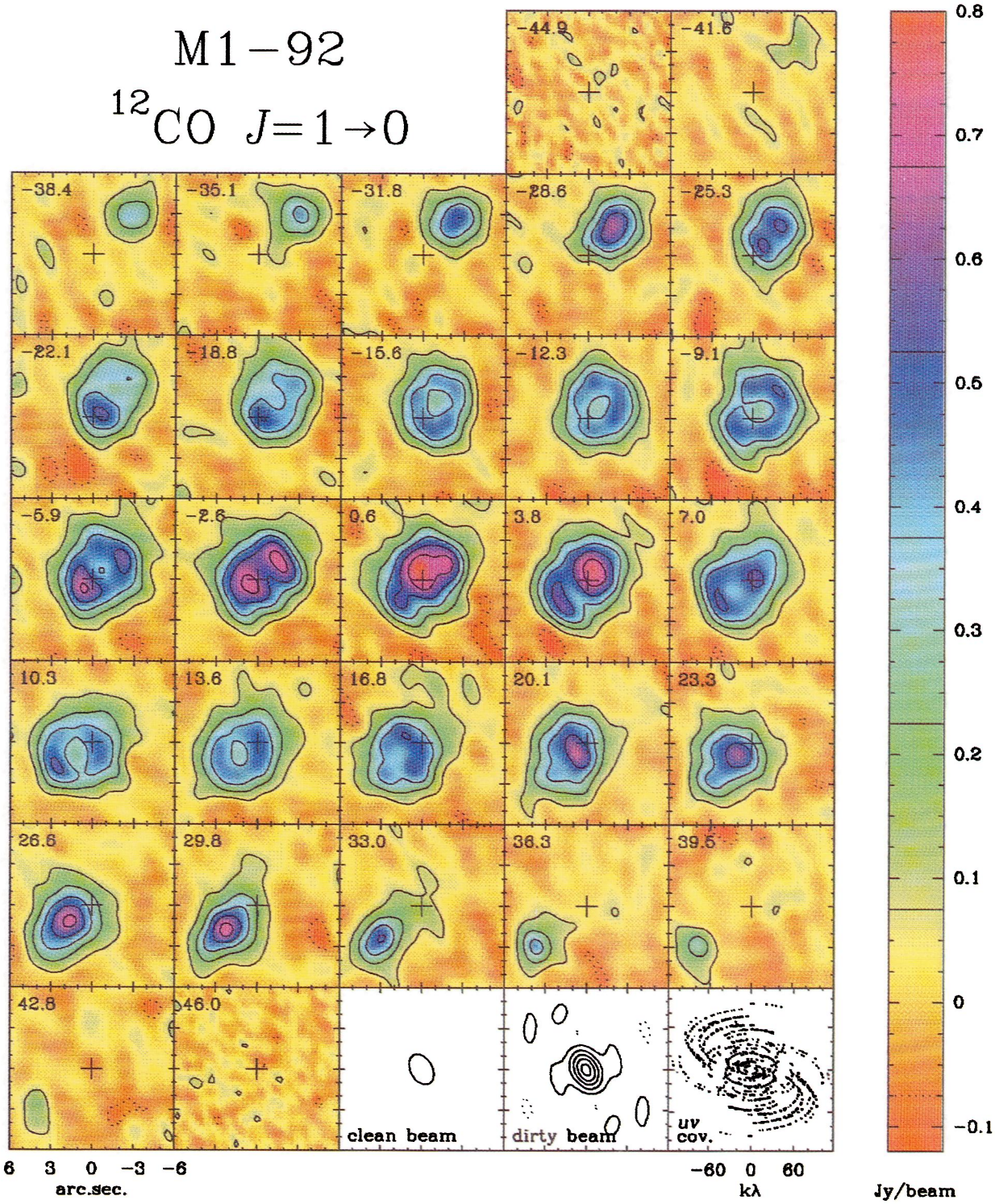

FIG. 1.—Maps of the CO 1–0 intensity for the LSR velocities indicated in the left-upper corners; up is north and left is east. The color and level scales are shown in the column, dashed lines represent negative contours. We also include the CLEANed beam (half-power contour), the dirty beam (contours from −10% to 90%, by intervals of 20%), and the *uv* coverage. Note the displacement of the emitting region along the symmetry axis with the velocity, and the presence of central holes for the intermediate velocities.

BUJARRABAL et al. (see 436, L169)

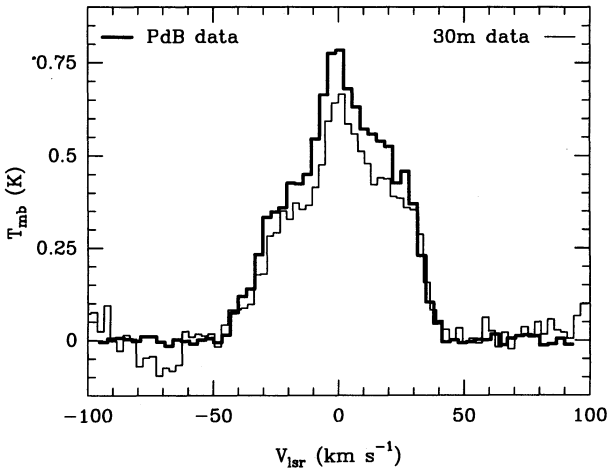

FIG. 2.—Single-dish profile of CO 1-0 from M1-92 obtained with the IRAM 30 m dish, and equivalent total synthetic profile from our interferometric data.

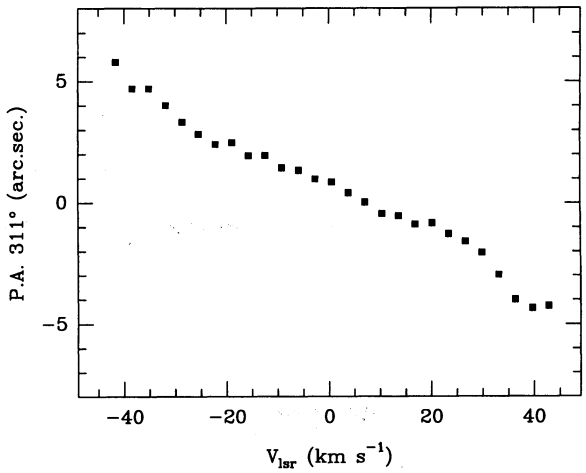

FIG. 3.—Position along the nebular symmetry axis of the CO emission centroid

janskys per beam. The number in the upper left corner of each panel shows the LSR velocity at the center of the corresponding channel. The r.m.s. noise in the maps is $\sim$40 mJy beam^{-1}. A synthetic total spectrum has been calculated by convolving the total emission with a 30 m telescope beam, to be compared with data obtained with the Pico de Veleta dish (Fig. 2). Both spectra are compatible, within the calibration uncertainties, so no significant flux is lost in the interferometric observations.

3. THE STRUCTURE OF M1-92

We have used the total synthetic spectrum of the ^{12}CO $J = 1$–0 transition (computed from our interferometric maps for a 30 m telescope beam; § 2, Fig. 2) to calculate the mass-loss rate of M1-92. We follow the method by Loup et al. (1993), expected to be reasonably accurate for circumstellar shells where the CO opacity is not extremely high. Since we are interested in an estimate of the total amount of molecular material, we neglect the structure of the profile. Assuming a distance of 3 kpc, a relative CO abundance of 3×10^{-4} (as for an O-rich envelope) and a representative expansion velocity of 30 km s^{-1}, we obtain an approximate mass-loss rate of $6 \times 10^{-5}\ M_{\odot}$ yr^{-1}. (This value is larger than that obtained for the OH-emitting region by Seaquist et al. [1991], following a very different method; the main reason for this disagreement is that these authors only consider a part of the shell.) The time necessary to eject the envelope is $\sim$2000–3000 yr, calculated either from representative observed CO extent and expansion velocity or from the parameters of the model given below. Therefore, a total mass of 0.1–0.2 $M_{\odot}$ was ejected, essentially during the AGB phase, to form the observed CO nebula. This amount of mass, determined from the molecular observations, is much larger than that deduced from the emission of (high- or low-excitation) atomic lines (Trammell, Dinerstein, & Goodrich 1993; Solf 1994), which is $\lesssim 10^{-2}\ M_{\odot}$. The bulk of the nebular material is then molecular, and properly probed by the CO observations.

In Figure 1 (Plate L10), we present the CO emission maps by velocity intervals of 3.25 km s^{-1}. The structure of the intensity distribution is particularly rich and distinct. The brightness distribution is remarkably symmetrical around the nebular axis, oriented at a position angle of 311°. A high degree of symmetry under inversion with respect to the central velocity and position is also found. In Figure 3 we represent the variation of the centroid of the emission along the (NW-SE) axis of symmetry, as a function of the LSR velocity. The total intensity (gray scale) and profile centroid (LSR velocity, in contours) are shown in Figure 4*a*, where a velocity-position map of the emission along the symmetry axis is also shown. Note that the whole structure presents a clear velocity gradient along this axis.

Our maps reveal the presence of three components in the molecular envelope of M1-92. First, for LSR velocities from -19 to 19 km s^{-1} we note the presence in each map of a central relative minimum, i.e., a hole (except for $V_{LSR} \sim 0$). In this velocity range, the position of the brightness centroid (which essentially is coincident with that of the central hole) varies with the velocity along the symmetry axis with a practically constant gradient (Fig. 3), over a total angular length of $\sim$5″. The intensity distribution remains similar for these intermediate velocities; consistent with a ring with outer and inner diameters of $\sim$5.″5 and 1.″5 (directly determined from a ring-fit to the visibilities). This intensity distribution seems to correspond to a mass distribution in a hollow prolate component, inclined toward the observer and with an axial velocity increasing with distance from the central star (as confirmed by the model presented below). At the end of this region of constant gradient in Figure 3, the velocity continues to increase but at a smaller rate. This behavior represents the kinematics of the two blobs detected at LSR velocities larger than $\sim$23 km s^{-1} in absolute value (Fig. 1). This structure is strongly bipolar and probably related to the fast bipolar outflow detected at other wavelengths. Finally, we note that no central decrease (but a conspicuous increase) of the CO emission is detected at the central velocity. This result indicates the presence of a central compact condensation (size $\sim$2″) with relatively low expansion velocity ($<$10 km s^{-1}), since it only occupies a small space in the position-velocity maps. We suggest that this clump is the inner part of the disk detected in IR and OH maser emission.

3.1. *A Model for the* CO *Emission from M1-92*

We have built a model for M1-92 consisting of the three different components above described. The density is assumed to decrease by a factor of 2 from the central compact clump to the hollow structure, and also from this one to the bipolar flow. A sketch of the assumed geometry and velocity field is represented in Figure 5. This velocity field has two components: a

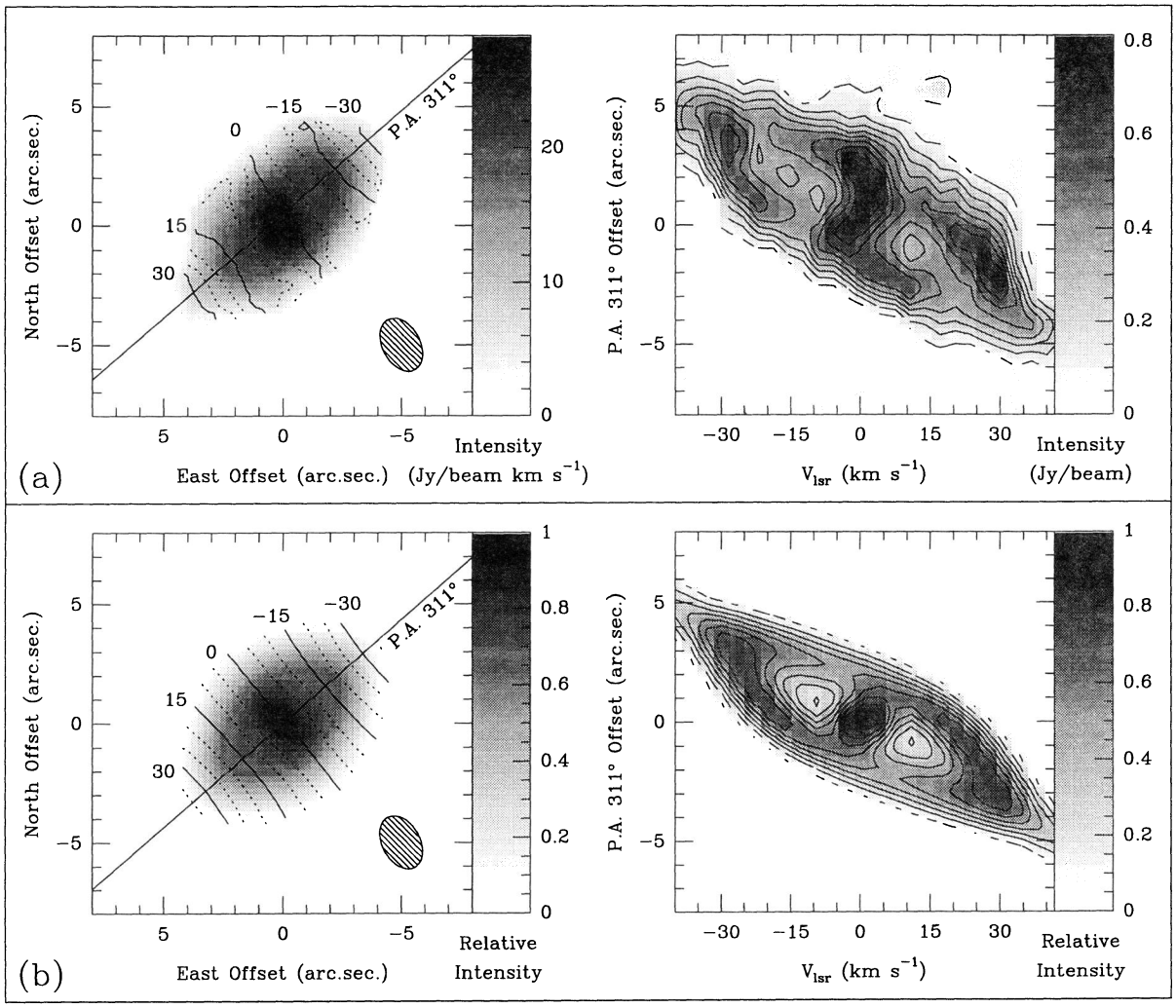

FIG. 4.—(*a*) CO observations of M1-92. *Left*: Maps of the velocity integrated intensity (*gray scale*) and velocity centroid (*contour scale*); the half-power contour of the CLEANed beam is shown by the hatched ellipse. *Right*: Intensity as a function of velocity and position along the symmetry axis. (*b*) Same as *a*, but for the predictions of our model for M1-92.

radial expansion, with a velocity of 5 km s^{-1} in the central clump and of 10 km s^{-1} in the rest of the nebula, and an axial velocity that increases proportionally to the distance from the equatorial plane up to $\sim$65 km s^{-1}. The inclination of the symmetry axis with respect to the plane of the sky is 35° (similar to the value given by Herbig 1975 and Solf 1994), with the NW blob pointing toward the observer. Note that the expansion velocity and size of the ring beyond our central clump are comparable to those of the torus assumed by Seaquist et al. (1991) to explain the OH emission (after correcting for the different inclination used by these authors). Also, two axial blobs with emission spectra in the visible similar to that of Herbig-Haro objects (separated by 5″–6″, Solf 1994) are placed just at the interface between our hole and CO shell. Finally, the optical reflection nebula fits in our CO whole structure.

Assuming optically thin emission and constant excitation in the CO line, we have calculated synthetic maps for the above model of M1-92, see Figure 4*b*. The agreement of the model results with the observations (Fig. 4*a*) is satisfactory, at least qualitatively. We think that our three-component model essentially accounts for the main characteristics of the molecular nebula in M1-92, although some observational features still remain to be explained. Note that our crude assumption of optically thin emission, that could be wrong at least for the intense emission of the central condensation, may lead to an underestimation of the density contrast between the different components. In our opinion, the main drawback of our modeling is the absence of hydrodynamical calculations, in order to propose consistent nebular structures. Such calculations, and a more accurate estimation of the resulting CO intensity, are in progress.

4. WIND INTERACTION IN PROTO–PLANETARY NEBULAE

The main result that can be extracted from our observations of M1-92 is the strong axial symmetry and the clear velocity increase with the distance along the symmetry axis. This is a model-independent result. The axial velocity reaches values up to $\sim$65 km s^{-1}. The continuity in the position-velocity maps of the different components (§ 3) is striking.

M1-92 was probably an AGB object in the past. The material ejected during this previous phase, that is expected to be still now the dominant component of the nebula, probably had a low expansion velocity, $\lesssim$10 km s^{-1}. This value is obtained from current data on AGB star envelopes and by the

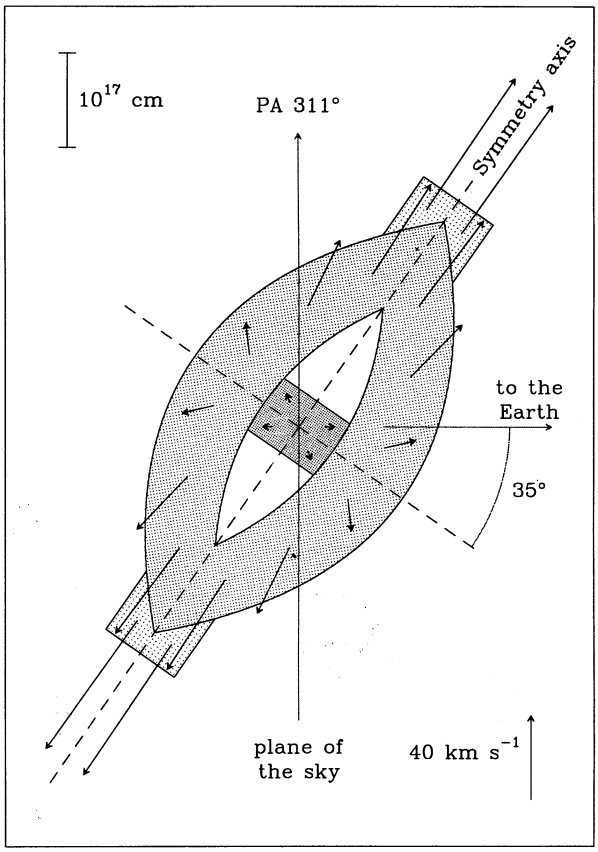

FIG. 5.—Sketch of the density distribution and velocity field of the model used for explaining our observations of M1-92.

present slow components of M1-92. Also note that AGB envelopes show in almost all cases a remarkable spherical symmetry. However, the molecular envelope of M1-92, a post-AGB object, shows now a strong axial distortion of the AGB symmetry, with a hollow shell of gas presenting a relatively high velocity (up to $\sim$60 km s^{-1}) in this axial direction. The fast bipolar flow, characteristic of protoplanetary nebulae, is also observed with a somewhat higher axial velocity. (We do not claim that the bipolar material observed in CO has been in fact ejected by the post-AGB star, it could have been accelerated by the fast, probably atomic gas ejected in this phase, but this does not affect our arguments.) Since no significant acceleration by radiation pressure is expected at such large distances to the star, the interaction between the AGB and the post-AGB winds is the only alternative to explain the complex structure observed in M1-92. The clear continuity in position and velocity between the bipolar component and the rest of the (disrupted) remnant of the AGB envelope in fact suggests a significant dynamical relation between the two flows, that involves most of the nebular material (at least 0.1 $M_\odot$) and strongly supports the wind interaction thesis. Such a dynamical interaction between the components must consist in the propagation of momentum from the bipolar fast flow, the only likely source of momentum in PPNs, to the rest of the nebula. We conclude that this phenomenon is active and very efficient in M1-92 at the present moment. We believe, in summary, that our molecular emission map of the Minkowski's Footprint is an instantaneous (observational) image of the wind interaction in PPNs, the process that very probably dominates the post-AGB circumstellar dynamics.

This work has been partially supported by DGICYT, project number PB 90-408.

REFERENCES

Calvet, N., & Cohen, M. 1978, MNRAS, 182, 687
Eiroa, C., & Hodapp, K.-W. 1989, A&A, 223, 271
Guilloteau, S., et al. 1992, A&A, 262, 624
Herbig, G. H. 1975, ApJ, 200, 1
Loup, C., Forveille, T., Omont, A., & Paul, J. F. 1993, A&AS, 99, 291
Seaquist, E. R., Plume, R., & Davis, L. E. 1991, ApJ, 367, 200
Solf, J. 1994, A&A., 282, 567
Trammell, S. R., Dinerstein, H. L., & Goodrich, R. W. 1993, ApJ, 402, 249